Rock Mech Rock Engng (2009) 42: 131–146
DOI 10.1007/s00603-009-0176-4
Printed in The Netherlands

Rock Mechanics and Rock Engineering

Improved Longitudinal Displacement Profiles for Convergence Confinement Analysis of Deep Tunnels

By

N. Vlachopoulos[1], **M. S. Diederichs**[2]

[1] Royal Military College, Ontario, Canada
[2] Queen's University, Ontario, Canada

Received December 2 2008; Accepted February 23 2009; Published online April 17 2009

Summary

Convergence-confinement analysis for tunneling is a standard approach for preliminary analysis of anticipated wall deformation and support design in squeezing ground. Whether this analysis is performed using analytical (closed form) solutions or with plane strain numerical models, a longitudinal displacement profile (LDP) is required to relate tunnel wall deformations at successive stages in the analysis to the actual physical location along the tunnel axis. This paper presents a new and robust formulation for the LDP calculation that takes into account the significant influence of ultimate (maximum) plastic radius. Even after all parameters are appropriately normalized, the LDP function varies with the size of the ultimate plastic zone. Larger yield zones take a relatively longer normalized distance to develop, requiring an appropriately calculated LDP. Failure to use the appropriate LDP can result in significant errors in the specification of appropriate installation distance (from the face) for tunnel support systems. Such errors are likely to result in failure of the temporary support. The equations presented here are readily incorporated into analytical solutions and a graphical template is provided for use with numerical modeling.

Keywords: Tunnelling, convergence-confinement, displacement, squeezing, ground reaction

1. Introduction

Convergence-confinement analysis (Duncan-Fama, 1993; Panet, 1993, 1995; Carranza-Torres and Fairhurst, 2000 and others) is a widely used tool for preliminary assessment of squeezing potential and support requirements for circular tunnels in a variety

Correspondence: M. S. Diederichs, Associate Professor, Queen's University, Ontario, Canada
e-mail: mdiederi@geol.queensu.ca

of geological conditions and stress states. The technique has been well documented and will not be discussed here in detail except to summarize the concept.

An analytical plasticity solution such as that developed by Carranza-Torres and Fairhurst (2000) is applied to a circular opening in an isotropic stress field. An internal pressure, initially equal to the in situ stress is applied on the inside of the excavation boundary. The pressure is incrementally relaxed until the excavation boundary condition is that of zero normal stress. The extent of plastic yielding and thereby, the boundary deformation is calculated at each stage of the process. The result is a continuous representation of the deformation-internal pressure relationship for the tunnel given a particular material strength, deformability, dilation and stress state.

The internal pressure is, of course not a representation of reality but rather a surrogate for the effect of the gradual reduction of the radial resistance provided by the initially present tunnel core (material inside the tunnel boundary) transitioning to an exposed boundary with a progressively distant tunnel face and ultimately a long open tunnel with plane strain conditions. The internal pressure that is coupled with a given boundary displacement is a measure of the amount of support resistance required to prevent further displacement at that point in the progressive tunneling model.

By making the significant and possibly debatable assumption that the support application does not change the material response, estimates of pressure-displacement

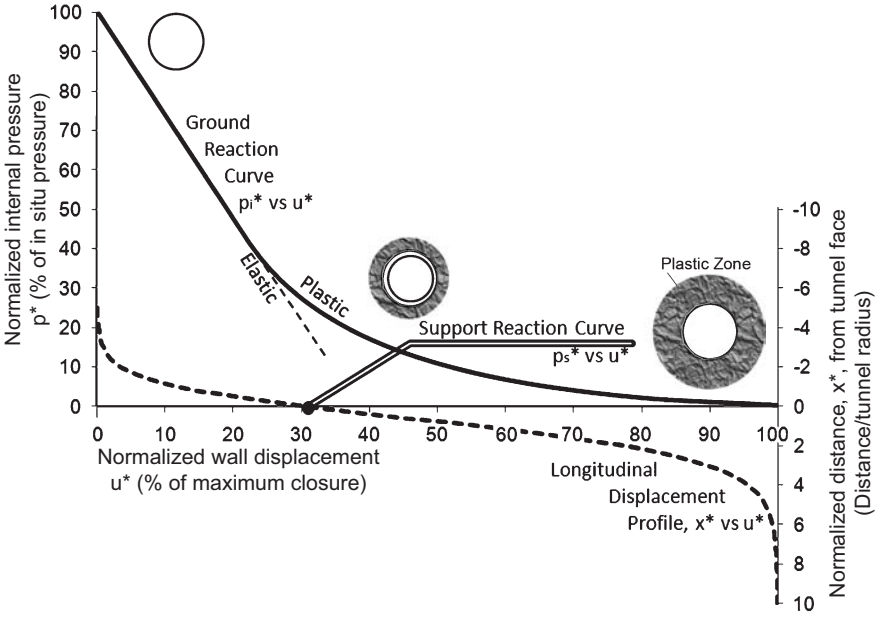

Fig. 1. Ground reaction (convergence confinement) curve shown with support reaction curve for liner installed at the tunnel face. The longitudinal displacement profile relates the normalized displacement to normalized location along the tunnel axis. Tunnel section is shown for elastic region, and for plastic zone development with and without support

curves can be compared to estimate the factor of safety against overload (Fig. 1). The support needs to be ''installed'' at the appropriate location (distance from the face). In order to calibrate the model so that the internal pressures or the displacements are correlated to a real distance from the face, a longitudinal displacement profile or LDP is required as shown in Fig. 1.

2. Longitudinal displacement profiles

In order to determine the appropriate timing for the installation of stiff support or when optimizing the installation of support with specific displacement capacity, for design purposes, it is important to establish the longitudinal closure or displacement profile for the tunnel. A portion of the maximum radial displacements at the tunnel boundary will take place before the face advances past a specific point. The tunnel boundary will continue to displace inwards as the tunnel advances further beyond the point in question. This longitudinal profile of closure or displacement versus distance from the tunnel face is called the longitudinal displacement profile or LDP. An example of a normalized LDP is shown in Fig. 1 and a tunnel specific (without normalization) LDP is illustrated in the example in Fig. 2.

The LDP cannot be calculated using 2D plane-strain models, although the LDP can be used to calibrate staged 2D models in which the inner tunnel core is replaced by incrementally relaxing boundary tractions to simulate a staged ground reaction

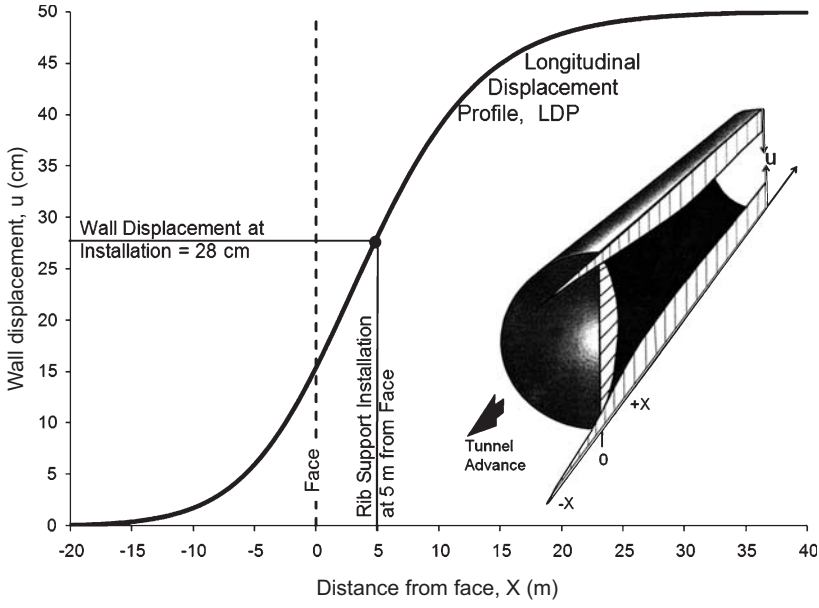

Fig. 2. Use of the longitudinal displacement profile, (LDP), to relate support installation location to nominal wall displacement for use in convergence–confinement ground/support reaction analysis. Schematic analysis based on a 10 m diameter tunnel at depth

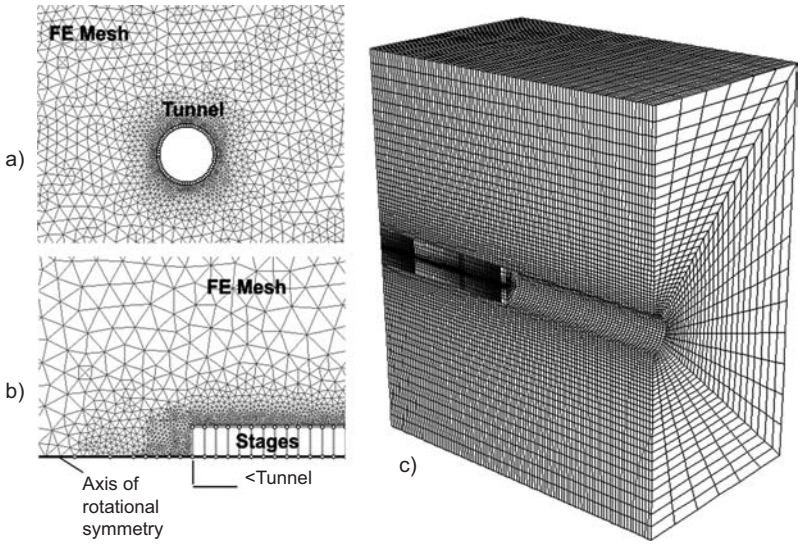

Fig. 3. Alternative approaches for tunnel modeling: a) 2D plane strain (PHASE2 – Rocscience, 2007) finite element model; b) axisymmetric finite element model with staged excavation; c) 3D finite difference model (FLAC3D – Itasca, 2006)

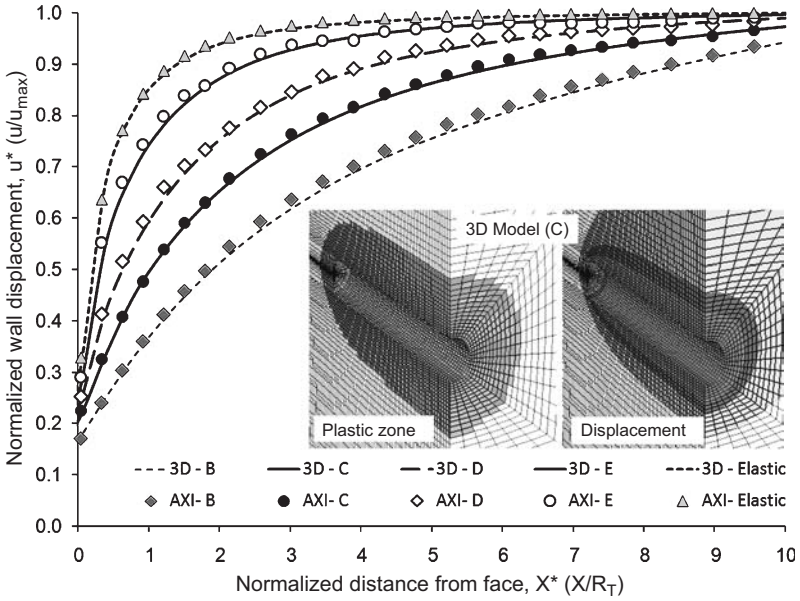

Fig. 4. Comparison between LDP's calculated using axisymmetric finite element models (Fig. 3b) and 3D finite difference models (Fig. 3c). An elastic analysis is shown and can be compared to plastic models with different ratios of isotropic in situ pressure p_0 and rockmass uniaxial compressive strength (UCS_{RM}). Materials B, C, D and E have p_0/UCS_{RM}, ratios of 8, 6, 4 and 2, respectively. Sample 3D results are shown in inset. The four tunnels are 5m in radius (R_T) and have maximum plastic radii (R_P) of approximately 26 m, 18 m, 12 m and 8 m, respectively

curve such as that shown in Fig. 1. A simple two-dimensional model (Fig. 3a) can be used to calculate the maximum wall displacement (u_{max}) and the maximum radius of the plastic (yielding) zone (R_P).

The LDP can be calculated using axisymmetric models for uniform or isotropic initial stress conditions and circular tunnel cross sections (Fig. 3b) of full three-dimensional models for complex loading and geometric conditions (Fig. 3c). This profile can be used to establish a distance-convergence relationship for 2D plane-strain modeling or for analytical solutions (as in Carranza-Torres and Fairhurst, 2000). For the simplified case of a circular tunnel in an isotropic stress field, a comparison between axisymmetric modeling and full 3D analysis (using FLAC3D – Itasca, 2006) is shown in Fig. 4.

There is an important caveat to consider when using numerical analysis to compute longitudinal displacement profiles. When using axisymmetric or full three-dimensional models to determine the longitudinal displacement profile relationship, it is important to consider the excavation rate. A stress front builds ahead of the bullet-shaped plastic zone and influences the rate of plastic zone development. Such models will yield a different apparent longitudinal displacement profile depending on the size of the excavation step. This is clearly shown in Fig. 5, where there is a significant difference between the instantaneous excavation and the 1 m (0.2D) step simulation (other excavation step sizes shown for comparison). For support sequencing, it is important to simulate the actual excavation step size or, if the tunneling is continuous (TBM), to use a small step size.

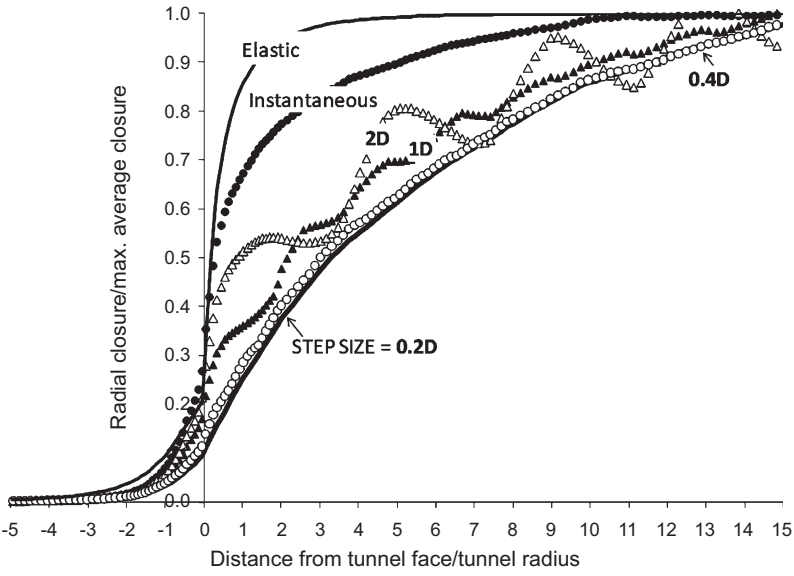

Fig. 5. Example of Influence of excavation step size (as a ratio of tunnel diameter D) on the modeled longitudinal displacement profile. Instantaneous excavation and elastic solution shown for comparison

3. Review of current LDP approaches

If only two-dimensional models are available or if an analytical convergence-confinement solution is to be used (as in Fig. 1), it is more practical to use an analytical function for the LDP. In order to facilitate analytical calculations of ground response (convergence-confinement), Panet (1995) derived a relationship for the longitudinal displacement profile based on elastic analysis:

$$u^* = \frac{u_R}{u_{\max}} = \frac{1}{4} + \frac{3}{4}\left(1 - \left(\frac{3}{3 + 4X^*}\right)^2\right) \tag{1}$$

where $X^* = X/R_T$, u_R is the radial displacement at a specified longitudinal position X, and $u_{\max}$ is the maximum short term radial displacement distant from the face and corresponding to plane strain analysis of a tunnel cross section. R_T is the tunnel radius and X is positive into the tunnel away from the face ($X = 0$). The position, X, is negative into the rock ahead of the face and is specified along the tunnel centerline.

Numerous other authors have suggested alternative expressions for the elastic longitudinal displacement profile including Unlu and Gercek (2003) who noted that the curve in front of the face and the curve behind the face do not follow a single continuous functional relationship with X. The authors agree with this assertion. The radial deformation profile with respect to distance from the face is accurately predicted for the elastic case to be:
for $X^* \leqslant 0$;

$$u^* = \frac{u_R}{u_{\max}} = \frac{u_0}{u_{\max}} + A_a\left(1 - e^{B_a X^*}\right) \tag{2a}$$

for $X^* \geqslant 0$

$$u^* = \frac{u_R}{u_{\max}} = \frac{u_0}{u_{\max}} + A_b\left(1 - (B_b/(A_b + X^*))^2\right) \tag{2b}$$

where u_0 is the radial displacement at the face location ($X^* = 0$) and A_a, A_b, B_a, B_b are functions of Poisson's Ratio:

$$\begin{aligned} u_0^* &= \frac{u_0}{u_{\max}} = 0.22\nu + 0.19; \\ A_a &= -0.22\nu - 0.19; \quad B_a = 0.73\nu + 0.81 \\ A_b &= -0.22\nu + 0.81; \quad B_b = 0.39\nu + 0.65 \end{aligned} \tag{3}$$

These preceding equations are for elastic deformation. Panet (1993, 1995), Panet and Guenot (1982), Chern et al. (1998) and other have proposed empirical solutions for longitudinal displacement profiles based on modeled plastic deformation of varying intensity (correlated to various indices such as the ratio between in situ stress and undrained cohesive strength, for example). Alternatively, an empirical 'best fit' to actual measured closure data can be used (for example, based on data from Chern et al., 1998):

$$u^* = \frac{u_R}{u_{\max}} = \left(1 + e^{\left(\frac{-X^*}{1.10}\right)}\right)^{-1.7} \tag{4}$$

These relationships are summarized in Fig. 6.

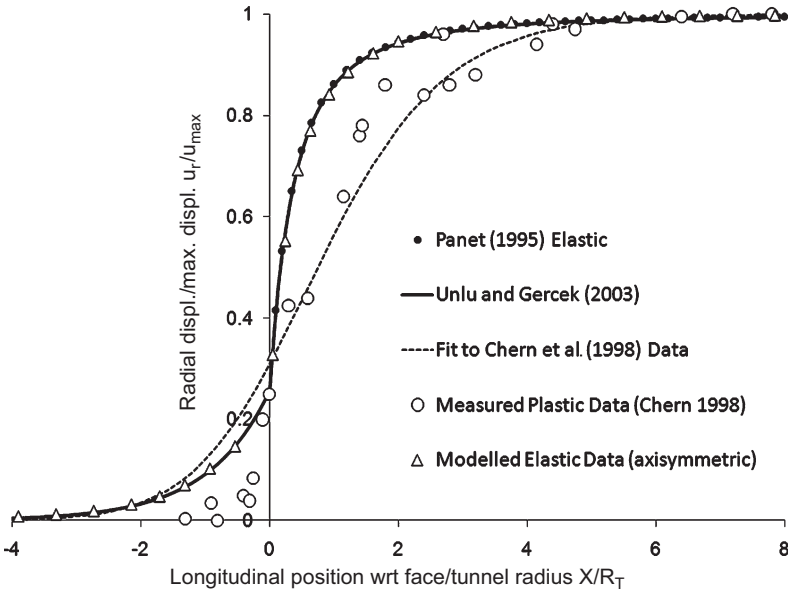

Fig. 6. Comparison of Longitudinal Displacement Profiles (LDP's) reported in the literature, including Eqs. (1) (Panet, 1995), (2) (Unlu and Gercek, 2003) and (4) (based on Chern et al., 1998)

4. Improved LDP related to plastic zone radius

The development of radial deformation, however, is directly linked to the development of the plastic zone as the tunnel advances. Studies by the authors have shown that the longitudinal displacement profile function proposed by Panet (1995) and by Unlu and Gercek (2003) is reasonable for plastic analysis provided that the radius of the plastic zone does not exceed 2 tunnel radii and provided that the yielding zone in the tunnel face does not interact with the developing yield zone around the tunnel walls as illustrated in Fig. 7.

The advancing front of plastic yielding is bullet shaped in three-dimensions and for large plastic zones (radius of plastic zone $R_P \gg 2 \times R_T$) the shape of this developing yield zone is geometrically similar for increasing maximum plastic radii. There is no reason, therefore, to expect that a single longitudinal displacement profile will suffice for these conditions. In order to account for the influence of increased overall yielding on the shape of the normalized longitudinal displacement profile, the most logical index to relate to the longitudinal displacement profile function is the normalized plastic zone radius, $R^* = R_P/R_T$.

To illustrate this problem, a series of analyses were performed involving a radial tunnel section and an axi-symmetric analysis along the tunnel axis. The first suite of analyses is based on a typical rockmass at 1100 m depth in a weak rockmass (e.g. graphitic phyllite). This is case A_1 in Table 1 below. In this case, the initial in situ stress is approximately 10 times the estimated rockmass uniaxial strength (UCS_{RM} or σ_{crm} calculated according to Hoek et al., 2002). Five other rockmasses are investigated

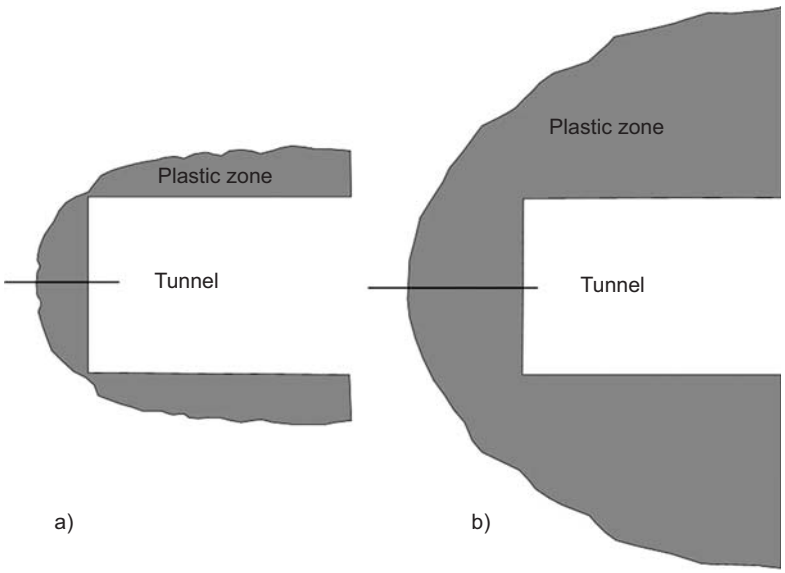

Fig. 7. a) Plastic yield zone developing as tunnel advances to the left (axisymmetric FEM analysis). Maximum plastic zone radius is less than twice the tunnel radius and the wall yield zone does not interact with the face yield zone (Panet's 1995 longitudinal displacement profile is valid); b) wall yield zone more than double the tunnel radius and interacts with face yield zone (Panet's longitudinal displacement profile is not valid)

Table 1. Rockmass parameters for longitudinal displacement profile analysis using PHASE2 (constant $p_0 = 28$ MPa)

	A_1	B_1	C_1	D_1	E_1	F_1	G_1
P_0/UCS_{RM}	10	8	6	4	2	1	Elastic
σ_{ci} (MPa)	35	35	35	50	75	100	
m_i	7	7	7	7	7	7	
ν	0.25	0.25	0.25	0.25	0.25	0.25	
GSI	25	35	45	48	60	74	
m	0.481	0.687	0.982	1.093	1.678	2.766	
s	0.0002	0.0007	0.0022	0.0031	0.0117	0.0536	
a	0.531	0.516	0.508	0.507	0.503	0.501	
E_{RM} (MPa)	1150	2183	4305	7500	11215	27647	1150
UCS_{RM} (MPa)	2.8	3.5	4.7	7	14	28	
P_0 (MPa)	28	28	28	28	28	28	28
R_T (m)	2.5	2.5	2.5	2.5	2.5	2.5	2.5

with increasing intact strength and/or *GSI* (Marinos and Hoek, 2000) giving a series of representative cases with varying p_0/UCS_{RM} (in situ stress/rockmass strength). The rockmass parameters are summarized in Table 1.

The rockmass strengths are estimated as per Hoek et al. (2002) and the elastic moduli are estimated based on Hoek and Diederichs (2006). A second set of analyses were performed based on rockmass A_1 (plastic) and G_1 (elastic) in Table 1 with increasing depth. The resultant in situ stress levels are listed in Table 2.

Table 2. Rockmass parameters for longitudinal displacement profile analysis using PHASE2 (constant $UCS_{RM} = 2.8$ MPa)

	A_2	B_2	C_2	D_2	E_2	F_2	G_2
P_0/UCS_{RM}	10	8	6	4	2	1	Elastic
P_0 (MPa)	28	22.4	16.8	11.2	5.6	2.8	28

Table 3. Summary results for tunnel with 2.5 m radius. R^* is the normalized plastic radius (R_P/R_T) while u_{max} is the maximum radial displacement

P_0/UCS_{RM}	10	8	6	4	2	1	Elastic
Constant P_0	A_1	B_1	C_1	D_1	E_1	F_1	G
R^*	7.5	5.1	3.5	2.3	1.5	1.2	1
u_{max} (m)	2.14	0.571	0.154	0.0495	0.0148	0.00367	0.0753
Constant UCS_{RM}	A_2	B_2	C_2	D_2	E_2	F_2	G
R^*	7.5	6.3	5.0	3.3	2.2	1.6	1
u_{max} (m)	2.14	1.25	0.632	0.242	0.0585	0.00167	0.0753

The tunnels were analyzed with Phase2 (Rocscience, 2007) in plane strain cross section to determine the extent of the plastic zone and the maximum radial deformation in each case. In addition, the cases were analyzed via axisymmetric models with 1 m incremental advance to determine the longitudinal displacement profile in each case as in Fig. 3b. The maximum displacements and plastic zone extents were comparable between the radial and longitudinal models. These summary results are presented in Table 3 and the resultant normalized longitudinal displacement profiles are presented in Fig. 8.

By inspection of Fig. 8 it is evident that the longitudinal displacement profile does not correlate with the stress/strength index p_0/UCS_{RM} as the set of curves in both plots represent the same selected values for this ratio and yet have different longitudinal displacement profiles. Analysis of the data, however, shows a direct correlation with the maximum normalized plastic zone, R_P/R_T, as expected. The correlation between u_0/u_{max} at $X/R_T = 0$ (at the face) and the maximum plastic radius, R_P/R_T, is shown in Fig. 9. Ignoring the influence of Poisson's ratio (negligible compared to plastic yielding) the best fit relationship (independent of material parameters and stress levels) is:

$$u_0^* = \frac{u_0}{u_{max}} = \frac{1}{3} e^{-0.15R^*} \tag{5}$$

where $R^* = R_P/R_T$.

The relationships proposed by Unlu and Gercek (2003) correctly illustrate that the behavior ahead of the face ($X < 0$ into the rockmass) does not follow the same continuous function as the behavior (progressive displacement) behind the face ($X > 0$ in the tunnel). Their functions summarized in Eq. (2), do not, however, capture the influence of a large developing plastic zone, nor does Eq. (1) by Panet (1995). Based on the analysis in the preceding discussion, a new set of relationships are presented here

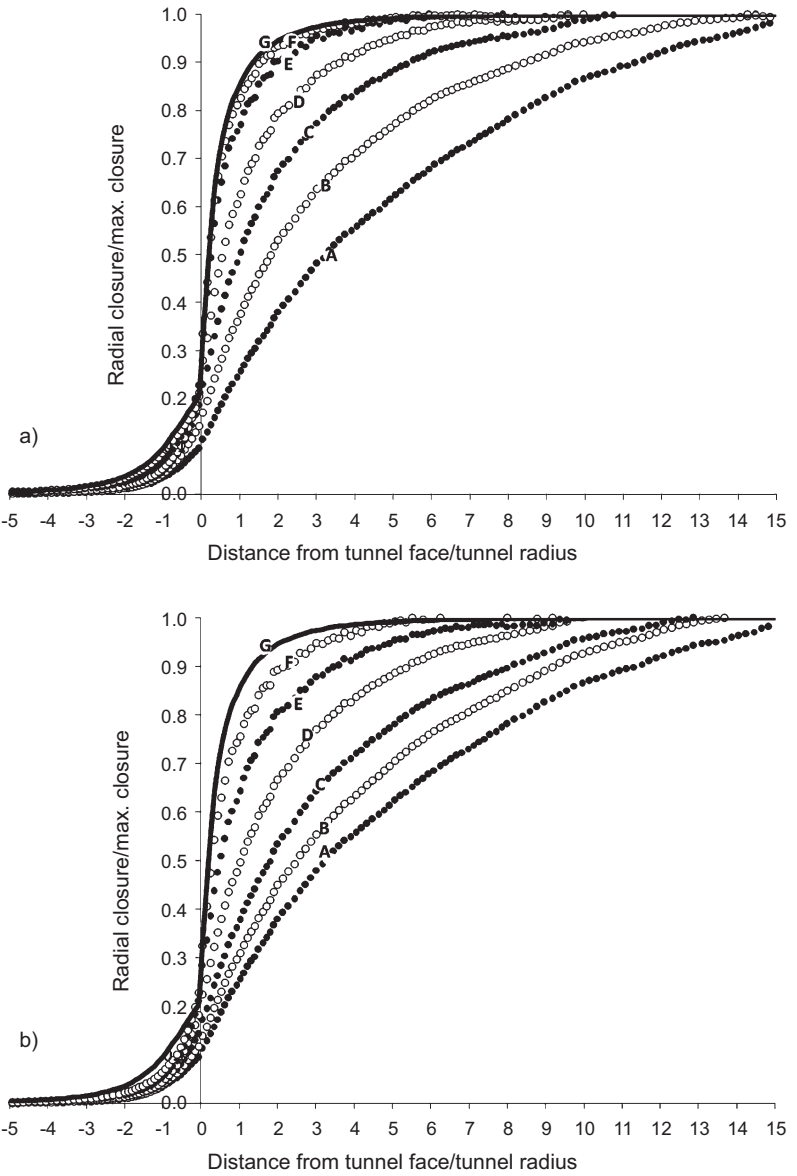

Fig. 8. Modeled longitudinal displacement profile results for axisymmetric models: a) constant p_0 model results; b) constant UCS_{RM} model. Labeled results (A–G) correspond to models in Table 3

that capture the influence of large plastic zone development on the longitudinal displacement profile. Best fit curves to the modeling results are shown in Fig. 10.

Equation (5) gives the relationship between normalized maximum plastic radius (at tunnel completion), R^*, and normalized closure $u_0^* = u_0/u_{\max}$ at the face ($X^* = 0$). Equations (6) and (7) give the best fit longitudinal displacement profile for $X^* \leqslant 0$ and

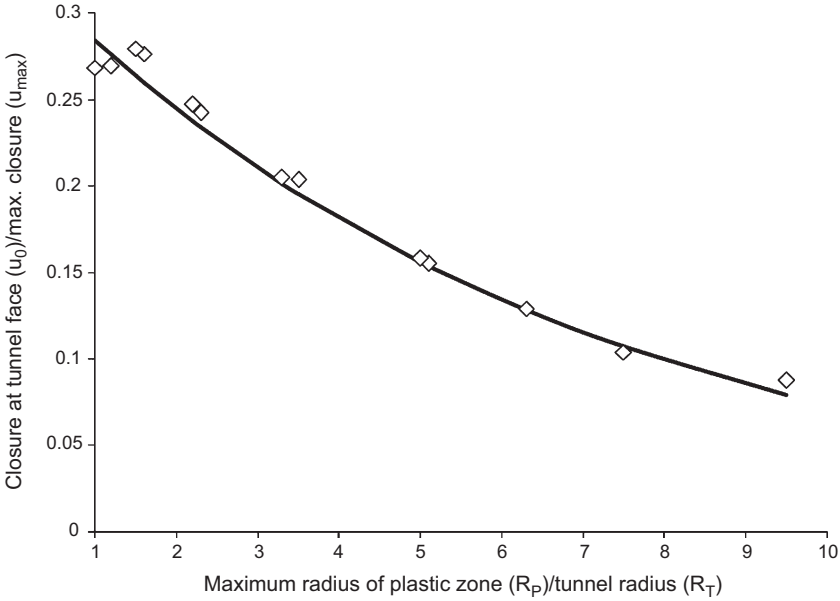

Fig. 9. Correlation between $u_0^* = u_0/u_{\max}$ at $X^* = X/R_T = 0$ (at the face) and the maximum plastic radius, $R^* = R_P/R_T$ for analyses in Table 3. Best fit relationship given in Eq. (5)

$X^* \geqslant 0$ as a function of normalized maximum plastic zone radius. The correlation with 2D model data is shown in Fig. 10.

$$u^* = \frac{u}{u_{\max}} = u_0^* \cdot e^{X^*} \quad \text{for} \quad X^* \leqslant 0 \text{ (in the rockmass)} \tag{6}$$

where $u_0^* = u_0/u_{\max}$ is given by Eq. (5).

$$u^* = 1 - \left(1 - u_0^*\right) \cdot e^{-\frac{3X^*}{2R^*}} \quad \text{for} \quad X^* \geqslant 0 \text{ (in the tunnel)} \tag{7}$$

where $R^* = R_P/R_T$.

5. Application

The new relationships summarized in Eqs. (5), (6) and (7) can be used to correlate displacement to position (along the tunnel) in order to accurately sequence support installation in staged 2D plane strain analyses (simulated tunnel advance through tunnel boundary relaxation). For 2D analysis, $u_{\max}$ and R_P need to be calculated prior to the sequenced analysis. The sequencing of the plane strain analysis can be accomplished through a core replacement technique (repeated replacement of the material within the tunnel core results in a force imbalance at the tunnel boundary that is resolved to equilibrium during subsequent convergence increment), or by progressively relaxing the tunnel boundary tractions from in situ to zero in stages. These two techniques are illustrated in Fig. 11. In these cases, the convergence axis values or the

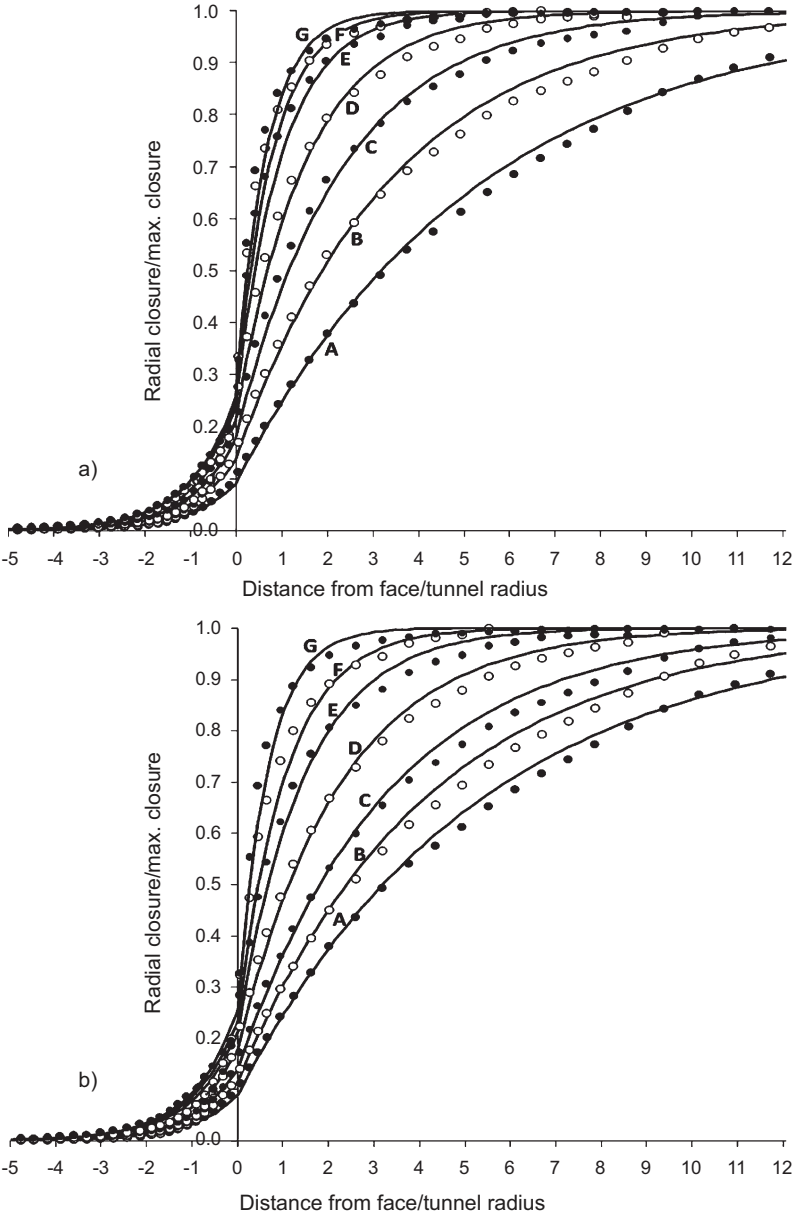

Fig. 10. Correlation between model data (from Table 3) and best-fit longitudinal displacement profiles (Eqs. (6) and (7)): a) constant p_0 analysis; b) constant UCS_{RM} analysis

convergence values at each analysis stage can be converted to location along the tunnel using the LDP obtained from Eqs. (5), (6) and (7).

The equations can be directly incorporated into convergence-confinement analysis as maximum displacement and maximum plastic zone radius are primary

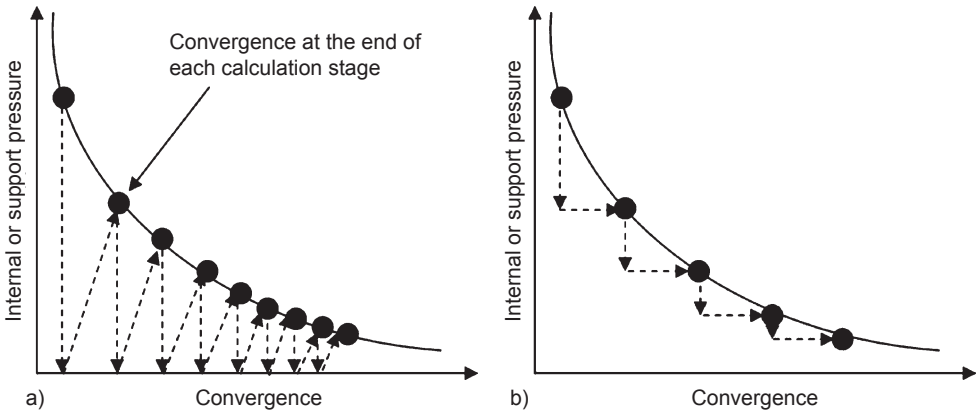

Fig. 11. Approaches for plane strain simulation of tunnel advance: a) replacement of tunnel core with unstressed elastic material (tunnel core reaction is shown as dashed line – core replacement results in a force imbalance which is resolved to equilibrium during subsequent convergence increment); b) incremental reduction (dashed line) of tunnel boundary tractions to simulate progressive advance

outputs of the analytical process. The convergence or normalized closure axis or analysis parameter can be converted using the LDP. The implications of using an elastic LDP (such as in Eq. (1)) in cases with large yield zones ($R^* > 2$) and wall convergence ($R^* > 2$) is illustrated in Fig. 12. In this example ($R_T = 5$ m,

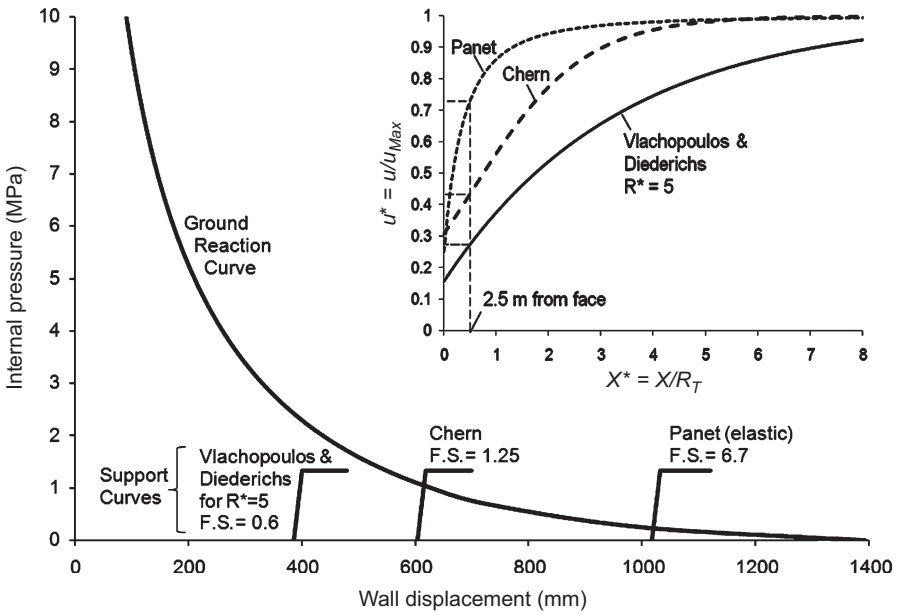

Fig. 12. Example comparison of Factor of Safety (F.S.) obtained through simple analytical convergence-confinement analysis using 3 different LDP's to guide support installation. Support (see text) is installed at 2.5 m from the face in all cases. $R^* = 5$ in this example

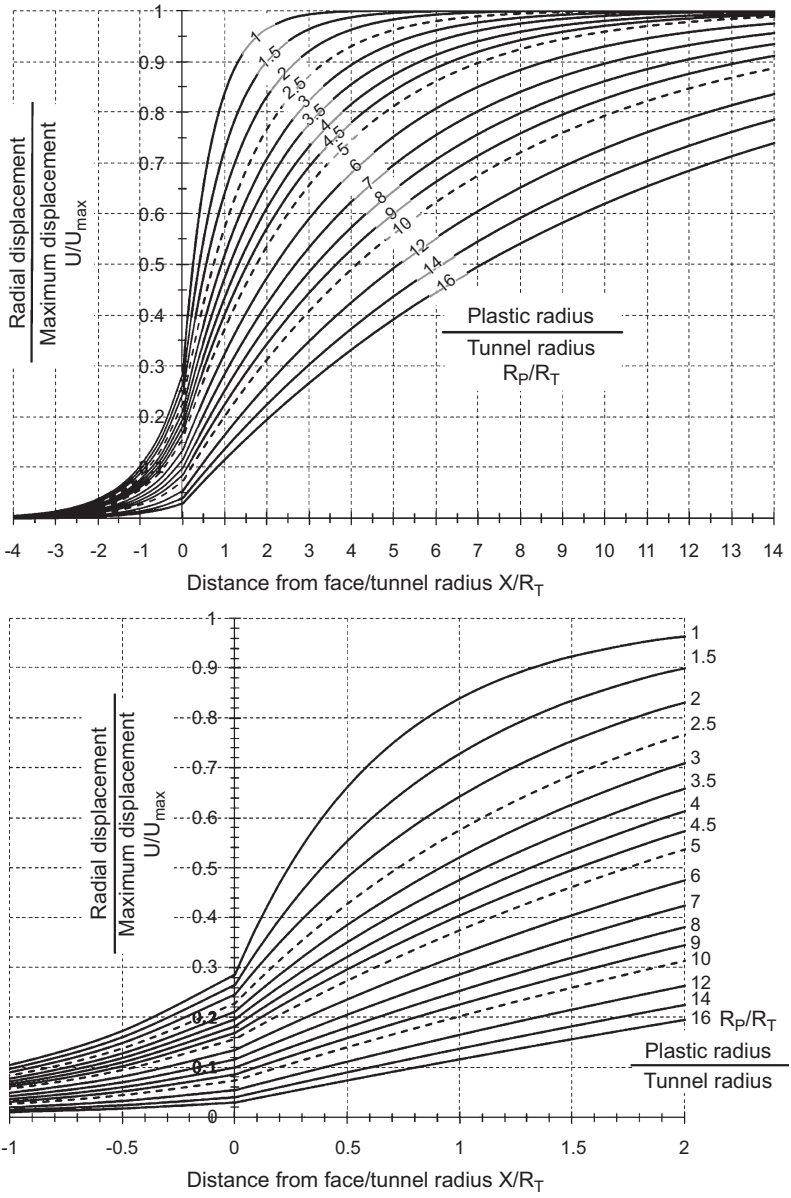

Fig. 13. LDP templates to be used as an alternative to Eqs. (5), (6) and (7). Lower plot is an expanded window on the near face region

$\sigma_{ci} = 30$ MPa, $GSI = 30$, Depth $= 1000$ m), the calculated maximum normalized plastic radius $R^* = 5$ and the maximum convergence, u_{max}, is 1.4 m (using the methology of Carranza-Torres and Fairhurst 2000 and elastic modulus estimation based on Hoek and Diederichs, 2006). In this example, a system of 20 cm I-Beam

arches at 0.5 m spacing is installed at a nominal 2.5 m from the face. The stiffness and capacity of this support system is calculated according to Hoek and Brown (1980).

If the elastically derived equation (''Panet'' for example) is used in this example the recommended timing of support installation (here shown with at 2.5 m or $X^* = 0.5$ giving a Factor of Safety of 6.7) will be erroneous and non-conservative. If the generic empirical formula (''Chern'') from Eq. (3) is used, the apparent Factor of Safety, for installation at 2.5 m, drops considerably to 1.25. If the LDP from Eqs. (5), (6) and (7) (''Vlachopoulos and Diederichs'') is used, then the Factor of Safety for installation at 2.5 m drops to 0.6 and support failure is predicted. Recommendation for completed support installation will be after significantly more convergence has taken place (possibly necessitating the use of sliding joints in the support rings as discussed in Shubert, 1996; Hoek et al., 2008).

The forgoing example is based on the assumption that the unsupported LDP can be used to appropriately locate the point of support installation. An alternative approach is to perform the analytical or numerical analysis with the design support pressure (reduced by the desired factor of safety). The final deformation, $u_{\max}$, and the final plastic radius, R_P, of the supported tunnel can be used in Eqs. (5), (6) and (7).

6. Conclusion

Using a series of numerical analyses, a new series of functions defining robust longitudinal displacement profiles, as a function of maximum normalized plastic radius, has been developed. This approach takes into consideration the effect that a large ultimate plastic radius has on the rate of development of wall displacements with respect to location along the tunnel. Previous LDP functions are inadequate for tunnel analysis in very week ground at great depth. This approach is valid from the elastic case through to complete plastic closure of the tunnel (as calculated using numerical or analytical solutions).

Equations (5), (6) and (7) define a relationship for a complete LDP ($X \leqslant \geqslant 0$) that can be incorporated directly into analytical solutions or used for calibration of staged numerical models. As an alternative to these equations, Fig. 13 provides a graphical template for this purpose. The equations and graphical tools presented here are for short term displacements occurring as a function of tunnel advance only. Where time-dependent squeezing is anticipated, this approach will need some modification following the guidance provided by Pan and Dong (1991). Care must be taken, in this case, to appreciate whether the time-dependent squeezing is accompaniedan increase in or is independent of the plastic radius.

Acknowledgements

Special thanks are due to Drs. Evert Hoek, Carlos Carranza-Torres, Brent Corkum and Giordano Russo for their insightful discussions on this topic as well We are also grateful to Matt Lato for early assistance with this work. This work has been funded by the Natural Science and Engineering Research Council of Canada as well as the Province of Ontario via the PREA program.

References

Carranza-Torres C, Fairhurst C (2000) Application of the convergence–confinement method of tunnel design to rock masses that satisfy the Hoek–Brown failure criterion. Tunn Undergr Sp Tech 15(2): 187–213

Carranza-Torres C, Diederichs MS (2008) Mechanical analysis of a circular liner with particular reference to composite supports – e.g., liners consisting of shotcrete and steel sets, Submitted for review and publication to Tunn Undergr Sp Tech (December 2007)

Chern JC, Shiao FY, Yu CW (1998) An empirical safety criterion for tunnel construction. Proceedings of the Regional Symposium on Sedimentary Rock Engineering, Taipei, Taiwan, pp 222–227

Duncan Fama ME (1993) Numerical Modeling of Yield Zones in Weak Rock. In: Hudson JA (ed) Comprehensive Rock Engineering, 2. Pergamon, Oxford, pp 49–75

Hoek E, Brown ET (1980) Underground Excavations in Rock. Institution of Mining and Metallurgy, London, 527 pp

Hoek E, Diederichs MS (2006) Empirical estimation of rock mass modulus. Int J Rock Mech Min Sci 43(2): 203–215

Hoek E, Carranza-Torres C, Corkum B (2002) Hoek-Brown criterion – 2002 edn. Proc. NARMS-TAC Conference, Toronto, 2002, Vol. 1, pp 267–273

Hoek E, Carranza-Torres C, Diederichs MS, Corkum B (2008) Kersten Lecture: Integration of geotechnical and structural design in tunnelling. Proceedings University of Minnesota 56th Annual Geotechnical Engineering Conference. Minneapolis, 29 February 2008, pp 1–53

Itasca (2006) FLAC3D. Version 3. Fast Lagrangian Analysis of Continua. 3D Version. www.itascacg.com

Marinos P, Hoek E (2000) GSI – A geologically friendly tool for rock mass strength estimation. Proc. GeoEng 2000 Conference, Melbourne, pp 1422–1442

Pan YW, Dong JJ (1991) Time-dependent Tunnel Convergence II. Advance Rate and Tunnel-Support Interaction. Int J Rock Mech Min SciGeomech 28(6): 477–488

Panet M (1993) Understanding deformations in tunnels. In: Hudson JA, Brown ET, Fairhurst C, Hoek E (eds) Comprehensive Rock Engineering, Vol. 1. Pergamon, London, pp 663–690

Panet M (1995) Calcul des Tunnels par la Me'thode de Convergence–Confinement. Presses de l'Ecole Nationale des Ponts et Chausse'es, Paris, 178 p

Panet M, Guenot A (1982) Analysis of convergence behind the face of a tunnel. Proceedings, International Symposium Tunnelling'82, IMM, London, pp 197–204

Rocscience (2007) PHASE2. 2D finite element software. www.rocscience.com

Schubert W (1996) Dealing with squeezing conditions in Alpine tunnels. Rock Mech Rock Engng 29(3): 145–153

Unlu T, Gercek H (2003) Effect of Poisson's ratio on the normalized radial displacements occurring around the face of a circular tunnel. Tunn Undergr Sp Tech 18: 547–553